JACS
JOURNAL OF THE AMERICAN CHEMICAL SOCIETY
Article
pubs.acs.org/JACS

High Efficiency Adsorption and Removal of Selenate and Selenite from Water Using Metal–Organic Frameworks

Ashlee J. Howarth,[†,∥] Michael J. Katz,[†,∥,⊥] Timothy C. Wang,[†] Ana E. Platero-Prats,[‡] Karena W. Chapman,[‡] Joseph T. Hupp,[†] and Omar K. Farha*[,†,§]

[†]Department of Chemistry, Northwestern University, 2145 Sheridan Road, Evanston, Illinois 60208-3113, United States
[‡]X-ray Science Division, Advanced Photon Source, Argonne National Laboratory, Argonne, Illinois 60439, United States
[§]Department of Chemistry, Faculty of Science, King Abdulaziz University, Jeddah 22254, Saudi Arabia

Supporting Information

ABSTRACT: A series of zirconium-based, metal–organic frameworks (MOFs) were tested for their ability to adsorb and remove selenate and selenite anions from aqueous solutions. MOFs were tested for adsorption capacity and uptake time at different concentrations. NU-1000 was shown to have the highest adsorption capacity, and fastest uptake rates for both selenate and selenite, of all zirconium-based MOFs studied here. Herein, the mechanism of selenate and selenite adsorption on NU-1000 is explored to determine the important features that make NU-1000 a superior adsorbent for this application.

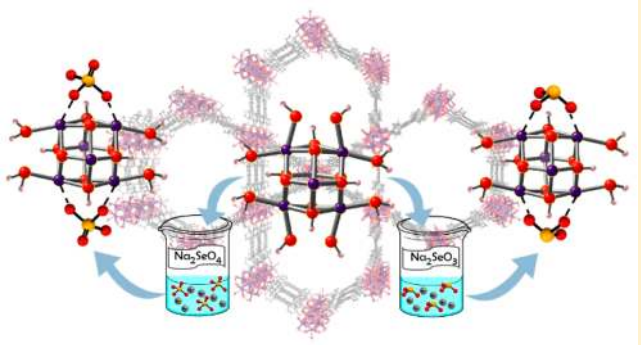

INTRODUCTION

Selenium is a naturally occurring element that is essential, in low concentrations, for human health. Of all essential elements however, selenium has the most confining range between dietary deficiency (<40 μg/day) and toxicity (>400 μg/day).[1] As a consequence of the narrow range between deficiency and toxicity, it is very important to monitor and control the amount of bioavailable selenium in our drinking water. Selenium enters our drinking water through a variety of sources, including agricultural runoff, mining, industrial production, and via flue gas desulfurization processes.[2] The U.S. Environmental Protection Agency (EPA) recognizes the dangers of selenium and has mandated a maximum acceptable level for selenium in drinking water of 50 ppb.[3] Selenium can occur in both organic and inorganic forms, but the high solubility and hence bioavailabilty of inorganic species such as selenite (SeO_3^{2-}) and selenate (SeO_4^{2-}) makes these anions the primary focus of remediation.[4]

Many approaches have been explored for the removal of selenite and selenate from water including the use of vertical flow wetlands[5] and bioreactors,[6] but the high startup costs and size requirements have limited the application of these techniques. An alternative approach that has been investigated involves using an adsorbing media to soak up and remove unwanted inorganic selenium.[7,8] Iron oxides (hematite, goethite and ferrihydrite) have been studied extensively as potential adsorbents for aqueous selenite and selenate. These materials have low surface areas, and the majority of the material is wasted due to the lack of available adsorption sites.[7] Furthermore, while the complexation that occurs between iron oxides and selenium oxyanions can differ based on pH, it is often found that iron oxides tend to be more effective for selenite removal due to the formation of inner-sphere complexes between the selenite anion and iron centers, which is a more difficult interaction to achieve with selenate, making its removal less effective.[7b,8]

We envisioned that metal–organic frameworks (MOFs) could offer an attractive alternative platform for adsorptive capture and removal of selenium-containing species. MOFs are structurally diverse, porous materials that are constructed from metal nodes bridged by organic ligands. Through careful ligand design, the chemical and physical properties of MOFs can be elegantly tuned and materials with very high surface areas,[9] high porosity, and high stability can be obtained.[10] As a consequence, MOFs have shown promise in a wide variety of potential applications, including catalysis,[11] sensing,[12] adsorption, storage, and release of gases,[13] as well as in the removal of toxic materials from air and water.[14] For adsorption applications, MOFs with permanent porosity can be designed and the size, shape, and chemical composition of the pores can be controlled to facilitate the uptake of specific guest molecules.[15] In terms of adsorption of contaminant/analyte molecules from aqueous solutions, MOFs containing zirconium metal nodes are of interest due to their inherent stability across a wide pH range in water.[16] This stability arises from the strong

Received: April 15, 2015
Published: May 22, 2015

DOI: 10.1021/jacs.5b03904
J. Am. Chem. Soc. 2015, 137, 7488–7494

Zr(IV)−O bonds, which also impart remarkable mechanical (external pressure up to 10 tons/cm^2)[16a,17] and thermal stability (decomposition temperatures >500 °C).[16a] In addition, it is well-known that hydrous zirconium oxides exhibit ion exchange behavior[18] and the affinity of Zr(IV) species for various oxo-anions, including selenate and selenite, has been well documented.[19] Given the presence of Zr-bound hydroxides in the nodes of many Zr-MOFs, we reasoned that anion exchange akin to that seen with zirconia can also occur in MOFs, but without the limitations of external-surface-only chemistry. Herein we explore the use of MOFs as an alternative technology for the removal of selenite and selenate anions from drinking water.

RESULTS AND DISCUSSION

Screening of Zr-Based MOFs for Adsorption of Selenate and Selenite. Metal−organic frameworks from the NU-1000 (Figure 1a), UiO-66 (Figure 1b), and UiO-67 families were screened for their selenate and selenite uptake ability. NU-1000 contains 8-connected Zr_6 nodes bridged by tetratopic pyrene-containing linkers to give the 3D structure shown in Figure 1a.[20] UiO-66 and UiO-67 contain 12-connected Zr_6 nodes bridged by 1,4-benzenedicarboxylate linkers (BDC) or biphenyl-4,4′-dicarboxylate linkers (BPDC), respectively (Figure 1b).[16a] Derivatives of UiO-66 containing BDC linkers functionalized with −NH_2 and −OH (Figure 1b) were also used to study how adsorption may be affected by the presence of different functional groups on the organic struts. For initial screening, two samples of each MOF were exposed separately to aqueous solutions of either selenate (100 ppm Se) or selenite (100 ppm Se). To allow sufficient time for adsorption to occur, solutions were first tested after 72 h of exposure and it was found that UiO-66 adsorbed 54% and 34% of the selenite and selenate present in the respective solutions (Figure 2). This suggests that anion exchange is occurring both on, and within, the MOF, demonstrating that Zr-bound hydroxides in a MOF are useful for adsorption of selenium oxo-anions, despite the strongly bridging nature of the OH group in the nodes of UiO-66. Furthermore, anion exchange appears to be enhanced by the presence of Lewis/Brønsted basic amine groups on the BDC linker with UiO-66-$(NH_2)_2$ and UiO-66-NH_2 (Figure 1b) showing some of the highest selenate and selenite adsorption per Zr_6-node among the MOFs studied (Figure 2). This is likely a consequence of hydrogen bonding interactions between the amine groups on the MOF linker and selenate and selenite anions. This type of adsorption would be similar to hydrogen bonding motifs in amine-containing macrocyclic frameworks which have been shown to have high affinities for sulfate and selenate anions.[21]

With these results in mind, and with the aim of enhancing uptake, we turned our attention to a MOF (NU-1000) that can more readily undergo anion exchange via substitution of nonstructural ligands.[22] Figure 2 shows that of the seven MOFs examined, NU-1000 achieves the highest degree of uptake of selenate as well as selenite, both gravimetrically and on a per-node basis. It also accomplishes the most complete removal of these ions from a 100 ppm Se test solution, i.e., 88% (SeO_4^{2-}) and 90% (SeO_3^{2-}). These results underscore the value and

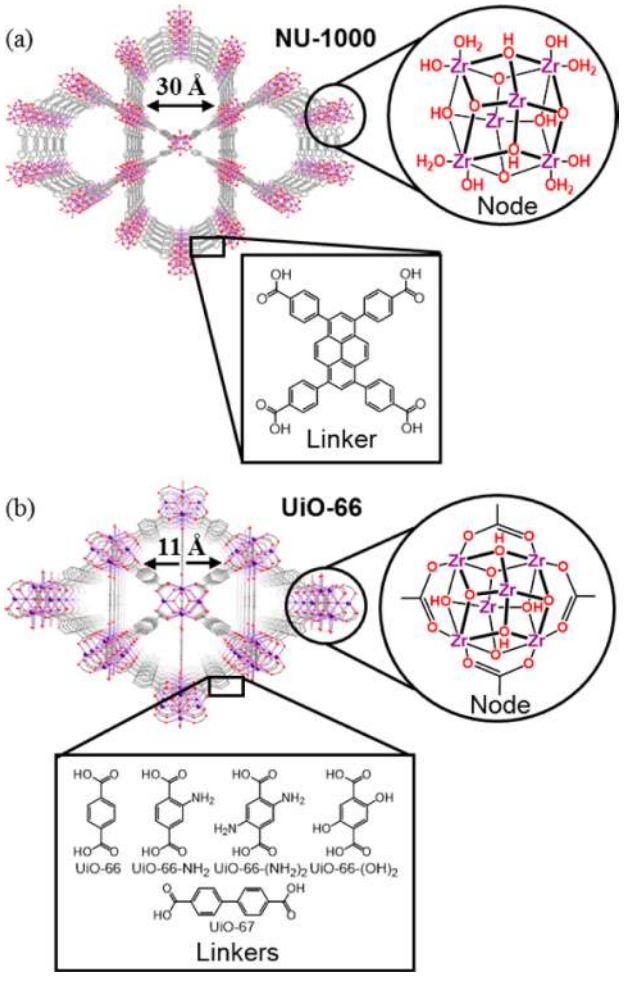

Figure 1. (a) Structure of NU-1000 highlighting the hexagonal pore size, the tetratopic linker, and the structure of the 8-connected Zr_6 node. (b) Structure of UiO-66 highlighting the octahedral pore size, the BDC linker, and derivatives used and the structure of the 12-connected Zr_6 node.

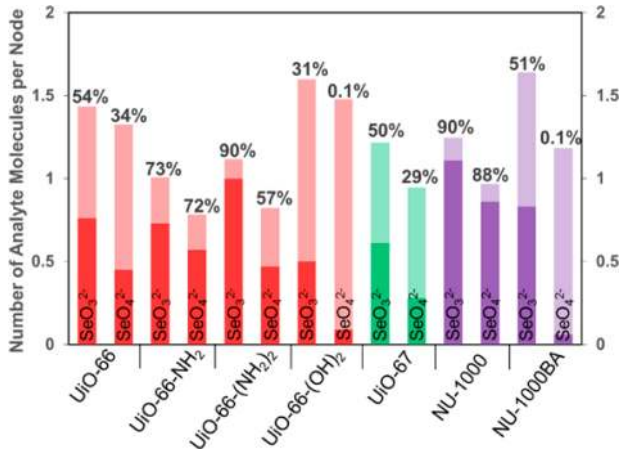

Figure 2. Bar graph illustrating the number of selenate or selenite molecules adsorbed per node in a series of Zr-based MOFs. Light colored bars in the back indicate the maximum possible per node adsorption based on the concentration of the solution (100 ppm Se; 5 mL, pH 7) and the amount of MOF present (10 mg). Dark colored bars indicate the actual per node adsorption calculated using the molecular weight of each MOF. For additional comparison, adsorption per node is given, above each bar, as a percentage of the maximum possible adsorption (i.e., the starting concentration of the solution used).

DOI: 10.1021/jacs.5b03904
J. Am. Chem. Soc. 2015, 137, 7488−7494

importance of MOFs with nonstructural-ligand lability in accomplishing anion uptake.

An alternative mode of uptake could conceivably be adsorption of the selenate/selenite sodium salt through, for example, oxy-selenium-anion/node-aqua(hydroxy) hydrogen bonding. ICP-OES (inductively coupled plasma-optical emission spectroscopy) measurements reveal no sodium adsorption in the MOF, indicating that the adsorbates cannot be salts, and implying that each adsorbed oxy-selenium dianion must be charge-balanced by loss of two anionic ligands (presumably hydroxides) from the MOF. ICP-OES measurements additionally established that no zirconium is lost to solution.

Given the high capacities of UiO-66-NH_2, UiO-66-$(NH_2)_2$, and NU-1000 for selenate and selenite, we also evaluated the kinetics of SeO_x^{2-} uptake. As shown in Figure 3, limiting high-

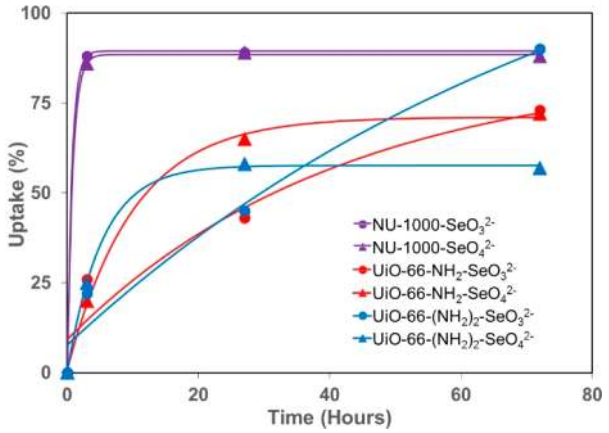

Figure 3. Kinetics of selenate and selenite uptake in NU-1000, UiO-66-NH_2, and UiO-66-$(NH_2)_2$. In each case, 10 mg of MOF was exposed to 100 ppm Se as selenate or selenite, respectively.

capacity uptake from 100 ppm solutions required 27 hours or more with UiO-66-$(NH_2)_2$ and UiO-66-NH_2, and less than 3 h with NU-1000. The faster uptake by NU-1000 compared with UiO-66 and its derivatives is likely related to aperture and pore size. NU-1000 has triangular and hexagonal pores which are 12 and 30 Å in diameter, respectively, with apertures of the same size (Figure 1a),[23] while UiO-66 comprises tetrahedral and octahedral pores that are 8 and 11 Å in diameter, respectively, with an aperture of 7 Å.[24] (Figure 1b shows the octahedral pore.) The apertures of UiO-66-NH_2 and UiO-66-$(NH_2)_2$ are anticipated to be even smaller. Selenate and selenite anions have diameters of 4.8[25] and 5.2 Å,[26] respectively. Therefore, based on pore size vs analyte size alone, one would expect diffusion of selenate and selenite through the pores of NU-1000 to be faster than diffusion within UiO-66 derivatives.

A notable feature of both NU-1000 and UiO-66-NH_2 is their ability to take up selenate and selenite with essentially equal efficacy. Many current technologies showing good responses toward selenite perform poorly toward selenate.[7] The ability to adsorb both forms of inorganic selenium is an important feature for selenium remediation. The high adsorption capacity combined with fast uptake time in NU-1000 suggest that both aperture size and the presence of substitutable ligands (aqua and hydroxy groups) on the Zr_6 node may be important for attaining high uptake capacity and fast uptake kinetics. Figure 4 summarizes the screening process for selenate and selenite adsorption in Zr-MOFs studied here.

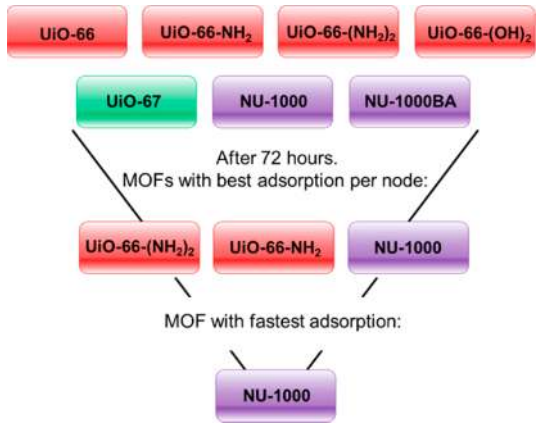

Figure 4. Flowchart outlining the screening process for selenate and selenite adsorption in Zr-based MOFs.

Mechanism of Selenate and Selenite Adsorption. To gain insight into the mechanism(s) of selenate and selenite adsorption on NU-1000, maximum adsorption capacities per Zr_6 node were determined. When exposed to aqueous solutions containing various concentrations of selenate and selenite anions ranging from 2 to 7 per node, the maximum number of anions adsorbed per node of NU-1000 was found to be two (Supporting Information Table S1). In addition, the affinities of NU-1000 for selenate and selenite are similar under these conditions, suggesting perhaps that the two analytes are bound in a similar fashion. At initial concentrations corresponding to more than six per node (>90 ppm Se for the solution volume and the amount of sorbent examined), NU-1000 is shown to take up more than two anions per node with concomitant adsorption of sodium cations. This adsorption of sodium shows that NU-1000 can no longer inherently charge balance when adsorption beyond two anions per node occurs. In the absence of Na^+ co-incorporation, for each doubly charged selenate or selenite anion adsorbed, two negative charges must be given up by the MOF to maintain charge balance. One way for NU-1000 to accommodate two selenate or selenite anions per node (−4 charge) would be to substitute all four terminal hydroxyl groups (OH^-) from the Zr_6 node; as detailed below, there is likely a substitution of water molecules as well (Figure 1a).

Diffuse reflectance infrared Fourier transform spectroscopy (DRIFTS) was used to gain insight into the location of the two analyte molecules per node of NU-1000. Prior to analyte adsorption, the IR spectrum of NU-1000 contains a sharp peak at 3670 cm^{-1} (Figure 5a,b, black trace) corresponding to stretching of the nodes' terminal −OH groups (Figure 1a).[20] The spectrum also contains a small peak at 2745 cm^{-1} (Figure 5a,b, black trace) corresponding to O−H stretches from hydrogen-bonding between the aqua and hydroxyl ligands in the Zr_6-node (Figure 1a).[20] After adsorption of ca. two molecules of selenate or selenite per node, the O−H stretch at 3670 cm^{-1} is greatly diminished and the hydrogen-bonding based O−H stretch at 2745 cm^{-1} disappears completely (Figure 5a,b, red and blue traces). On the basis of this information, it is reasonable to suggest that each SeO_4^{2-} or SeO_3^{2-} anion replaces two terminal hydroxyl groups on the Zr_6-node. Therefore, when two analyte molecules are bound per node, all four terminal hydroxyl groups are replaced and analyte binding can occur in a $\eta_2\mu_2$ or μ_2 fashion (Figure 5c).

Pair distribution function (PDF) analyses of X-ray total scattering data were used to evaluate the structural changes

DOI: 10.1021/jacs.5b03904
J. Am. Chem. Soc. 2015, 137, 7488−7494

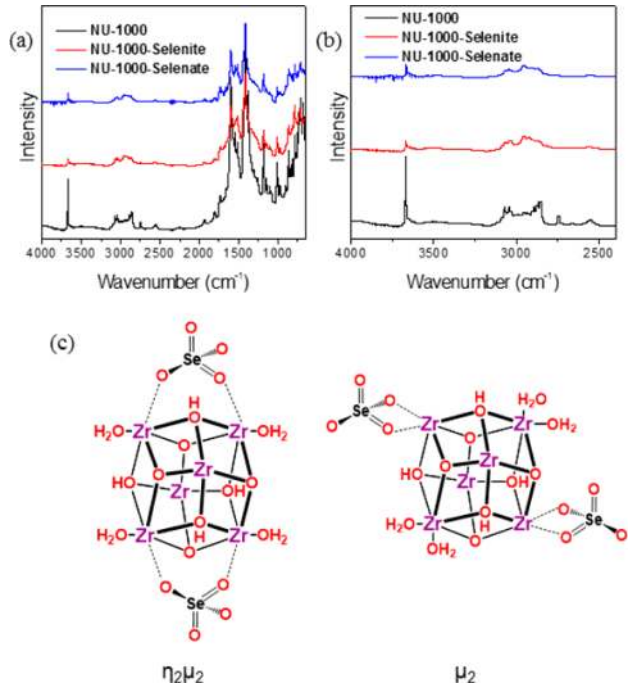

Figure 5. (a) DRIFTS spectrum of as-synthesized NU-1000 (black trace) and NU-1000 after adsorption of two molecules of selenite (red trace) and selenate (blue trace). (b) DRIFTS spectrum blown up from 4000 to 2000 cm^{-1}. (c) Potential binding modes of selenate (or selenite) to the node of NU-1000.

accompanying binding of selenate and selenite anions. Simulated PDFs indicate Se−Zr distances of 3.41 and 2.72 Å, respectively, for $\eta_2\mu_2$ and μ_2 binding (Figure 6a). The

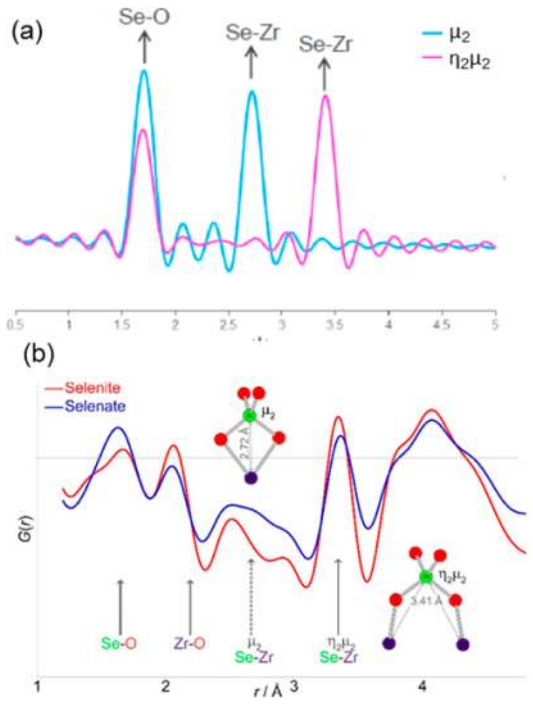

Figure 6. (a) Calculated differential PDFs for selenite and selenate-loaded NU-1000. (b) Experimental differential PDFs for selenite and selenate-loaded NU-1000 only showing peaks at distances matching $\eta_2\mu_2$ binding.

experimental PDF results, evaluated from difference data so as to isolate atom−atom distances unique to the adsorbent/adsorbate combination, showed a feature at ∼3.4 Å (3.36 Å for selenite, 3.37 Å for selenate), but not at 2.7 Å, clearly indicating that these anions exclusively bind in an $\eta_2\mu_2$ mode (Figure 6b). Both differential PDFs show peaks at ∼1.7 Å assignable to the Se−O distance within the anion, and features at 2.0−2.3 Å consistent with a slight contraction of the average Zr−O distance.

Adsorption Behavior of NU-1000 at Low Concentration of Selenate and Selenite. To test if current EPA standards for selenium in water can be satisfied by using NU-1000 as a sorbent, uptake of selenate and selenite at low concentrations was also studied. When exposed to 5 mL of an aqueous solution of selenium as sodium selenite or sodium selenate at 1000 ppb, 2 mg of NU-1000 adsorbed 98% of the selenite or selenate in solution in less than 5 min (Supporting Information Figure S1). After 3 h, the amount adsorbed remained constant, meaning that the anions adsorbed after 5 min did not subsequently leach from the sorbent. With a remnant solution concentration of only ∼20 ppb selenium, test samples treated with NU-1000 meet the EPA standards for drinking water of <50 ppb selenium.[3] Adsorption of selenate and selenite by NU-1000 at low concentrations was also tested at 40 °C (Supporting Information Figure S2) and pH 6 (Supporting Information Figure S3) to simulate the conditions of recirculating cooling water from the flue gas desulfurization process in power plants where selenate and selenite remediation is a concern.[27] The successful tests showed that NU-1000 is a promising candidate for removal of selenite or selenate under power plant operating conditions.

Adsorption Capacity of NU-1000. The amount of selenite and selenate adsorbed per gram of NU-1000 was probed by exposing the MOF to various concentrations of selenite or selenate and monitoring the amount adsorbed (q) in milligram of analyte per gram of adsorbent over time (Figure 7). Adsorption isotherm data was fit using the Langmuir model, and high correlation coefficients were obtained (Supporting Information Figure S4 and Table S2). With the use of the Langmuir equation, the maximum adsorption capacity (Q) of NU-1000 for selenite is 95 mg/g and for selenate is 85 mg/g. At amounts (i.e., concentrations and volumes) corresponding to 1.00−3.00 selenite or selenate anions per Zr_6 node, NU-1000 was found to reach its maximum adsorption within 1 min of exposure (Figure 7). The adsorption capacity of NU-1000 places it among the highest-capacity selenate and selenite adsorbing materials described to date (Supporting Information Table S3).[28] The uptake time of < 1 min sets NU-1000 apart from other materials such as aluminum oxide[28a,b] and iron oxide[28a−c] derivatives as well as ion exchange[28d] and polymer resins,[28e] each of which requires 30 or more minutes to reach maximum adsorption capacity under equivalent conditions.

Post-Adsorption Characterization of NU-1000. Characterization of NU-1000 before and after adsorption of selenate and selenite suggests that the framework remains intact. Powder X-ray diffraction patterns are unchanged before and after adsorption (Supporting Information Figure S5a). The Brunauer−Emmett−Teller (BET) volumetric surface area of NU-1000 before adsorption is 1035 ± 5 m^2/cm^3 (gravimetric surface area: 2130 ± 5 m^2/g), whereas after adsorption of selenate and selenite, the volumetric surface area drops slightly to 682 ± 10 and 705 ± 10 m^2/cm^3, respectively (gravimetric surface area: 1240 ± 10 and 1300 ± 10 m^2/g) (Supporting

DOI: 10.1021/jacs.5b03904
J. Am. Chem. Soc. 2015, 137, 7488−7494

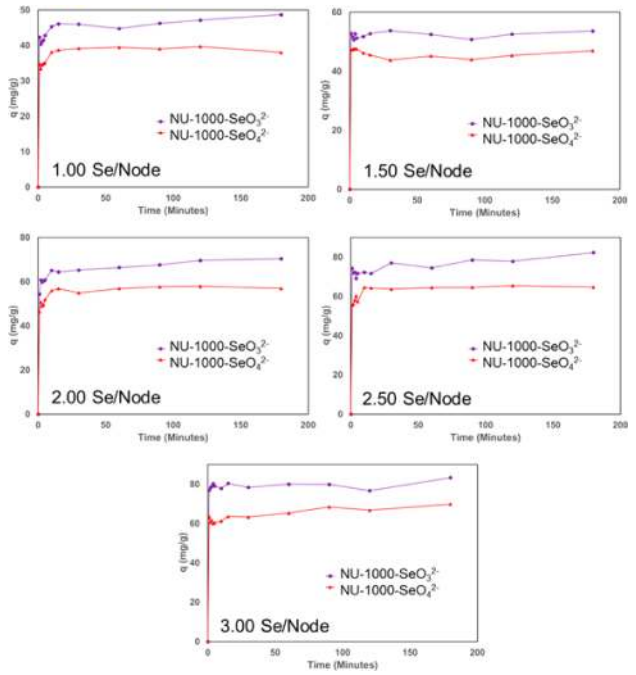

Figure 7. Amount adsorbed (q) vs time at various concentrations of selenate and selenite per node of NU-1000.

Information Figure S5b). Similarly modest decreases have been reported following Al(III) installation on NU-1000's nodes via atomic layer deposition.[23] SEM-EDX analysis performed on NU-1000 after adsorption of selenate and selenite show that Se is evenly distributed throughout the MOF, confirming that adsorption occurs on and in the framework (Supporting Information Figure S6).

CONCLUSION

In summary, adsorption of aqueous selenate and selenite by a series of highly porous, water stable, Zr-based MOFs has been explored. Of the seven MOFs examined, NU-1000 was found to exhibit both the highest gravimetric adsorption capacity and fastest rate of uptake. The results point to the importance of both large MOF apertures and substantial numbers of node-based adsorption sites, i.e., substitutionally labile Zr(IV) coordination sites, for rapid and effective selenate and selenite adsorption and removal to occur. Both anions are shown to bind to the node in a bridging ($\eta_2\mu_2$) fashion where one dianion bridges two zirconium metal centers. In contrast to many materials and associated technologies for selenium remediation, which are reasonably effective only for selenite,[7b,29] NU-1000 displays a strong affinity for both selenate and selenite. Given the vast library of metal nodes and organic linkers that have been used to construct MOFs with various aperture sizes and properties, there are many MOFs in the literature that contain functionalities that may prove to be useful for the adsorption of selenate, selenite, and other harmful oxyanions with a prerequisite of water stability. For example, since iron oxides have been shown to adsorb selenium oxyanions,[7,8] the use of iron-containing MOFs may also be of interest, particularly those consisting of Fe nodes bearing terminal hydroxyl and water groups which are substitutionally labile.[33] The high surface areas, permanent porosity, stability, and excellent tunability of MOFs makes these materials compelling candidates for adsorption applications and water remediation.

METHODS

General Experimental. UiO-66, UiO-66-NH_2, UiO-66-$(NH_2)_2$, UiO-66-$(OH)_2$, and UiO-67 were made according to literature procedures.[16c] NU-1000 was made according to a recently published, modified procedure.[20] Powder X-ray diffraction measurements were obtained using a Bruker MX $I\mu$S microsource with Cu Kα radiation and an Apex II CCD detector. Measurements were made over a range of $2° < 2\theta < 37°$. N_2 adsorption and desorption isotherm measurements were performed on a Micromeritics Tristar II at 77 K. Samples were activated by heating at 120 °C for 12 h under high vacuum on a Micromeritics Smart VacPrep. All gases used were Ultra High Purity Grade 5 as obtained from Airgas Specialty Gases. DRIFTS were recorded on a Nicolet 6700 FTIR spectrometer equipped with an MCT detector that was cooled to 77 K. The spectra were collected in a KBr mixture under Argon purge (samples prepared in air). Pure KBr was measured as the background and subtracted from sample spectra. ICP-OES data were collected on a Varian Vista MPX ICP Spectrometer. ICP-MS data were collected on a ThermoFisher X Series II instrument equipped with Collision Cell Technology (CCT) to reduce interferences from doublets for accurate detection of Se. ICP standards were purchased from Fluka Analytical. The as-purchased Na and Se ICP standards were 1000 mg/L in 2% nitric acid, TraceCERT and the Zr standard was 10 000 μg/mL in 4 wt % HCl. Standards for ICP-OES measurements (0.25−10 ppm) were prepared via serial dilution in 3% H_2SO_4, and standards for ICP-MS measurements (4−1000 ppb) were prepared via serial dilution in 3% HNO_3. Scattering data for PDF analysis were collected at beamline 11-ID-B at the Advanced Photon Source (APS) at Argonne National Laboratory (ANL). High energy X-rays (58.66 keV, λ = 0.2114 Å) were used in combination with a Perkin-Elmer amorphous silicon-based area detector. The samples were loaded into Kapton capillaries for PDF measurements under ambient conditions. PDF measurements were collected on NU-1000 samples containing selenate or selenite by taking 60 frames of 2 s exposure each. The 2-D scattering images were integrated to obtain 1-D scattering intensity data using software Fit2D.[30] The structure function $S(Q)$ was obtained within software PDFgetX3.[31] Direct Fourier transform of the reduced structure function $F(Q) = Q[S(Q) - 1]$ led to the reduced pair distribution function, $G(r)$, with Q_{max} = 23 Å^{-1}. Contributions from the pristine MOF were measured under exactly same conditions and subtracted to yield differential PDF (dPDF). The dPDF data show the new contributions coming from Se-atom correlations. Models for Se coordination modes ($\eta_2\mu_2$ or μ_2) to the MOF Zr-cluster were constructed within CrystalMaker. PDFs for both models were simulated using PDFGui[32] and compared with the experimental ones.

Initial Uptake Studies. Initial selenite/selenate uptake studies were performed by exposing 10 mg of MOF to 5 mL of an aqueous, 100 ppm solution of selenium as sodium selenite or sodium selenate in a 15 mL polypropylene centrifuge tube. In addition, 100 ppm control solutions of sodium selenite and sodium selenate were also prepared. The solutions were centrifuged for 1 min to allow the MOF to settle to the bottom of the tube. After 72 h, 0.5 mL of the supernatant was removed and diluted to 10 mL in 3% H_2SO_4 for ICP-OES measurements. ICP-OES was used to determine the concentration of Se, Zr, and Na in each solution. Comparison of control solutions to those containing MOF was used to determine the amount of selenate or selenite adsorbed by the MOF.

Kinetic Screening. Kinetic studies were performed by exposing 10 mg of UiO-66-$(NH_2)_2$, UiO-66-NH_2, and NU-1000 to 5 mL of an aqueous, 100 ppm solution of selenium as sodium selenite or sodium selenate in a 15 mL polypropylene centrifuge tube. The solutions were centrifuged for 1 min to allow the MOF to settle to the bottom of the tube. Then, 0.5 mL aliquots of the supernatant were removed at 3, 27, and 72 h and diluted to 10 mL in 3% H_2SO_4 for analysis by ICP-OES. ICP-OES was used to determine the concentration of Se, Zr, and Na in each solution. Comparison of control solutions to those containing

DOI: 10.1021/jacs.5b03904
J. Am. Chem. Soc. 2015, 137, 7488−7494

MOF was used to determine the amount of selenate or selenite adsorbed by the MOF at each time.

NU-1000 Maximum Uptake Per Node. The maximum uptake per node of NU-1000 was determined by exposing 2 mg of NU-1000 to 5 mL of an aqueous solution of sodium selenite or sodium selenate in a 15 mL polypropylene centrifuge tube with selenium concentrations of 30, 45, 60, 75, 90, and 105 ppm. These concentrations correspond to an exposure level of 2−7 analyte molecules per MOF node (i.e., Zr_6 cluster). The solutions were centrifuged for 1 min to allow the MOF to settle to the bottom of the tube. Aliquots of the supernatant were removed and diluted to 10 mL in 3% H_2SO_4 for analysis by ICP-OES. ICP-OES was used to determine the concentration of Se, Zr, and Na in each solution. Comparison of control solutions to those containing MOF was used to determine the number of selenate or selenite anions adsorbed per node of NU-1000.

NU-1000 Uptake at Low Concentrations. Low concentration kinetic studies were performed by exposing six 2 mg samples of NU-1000 to 5 mL of an aqueous, 1 ppm solution of selenium as sodium selenite or sodium selenate in a 15 mL polypropylene centrifuge tube. The solutions were centrifuged for 1 min to allow the MOF to settle to the bottom of the tube. Then, 2895 μL aliquots of the supernatant were removed from each solution at different times (5, 10, 15, 30, 60, and 180 min) and diluted to 3 mL in 3% HNO_3 for analysis by ICP-MS. ICP-MS was used to determine the concentration of Se, Zr, and Na in each solution. Comparison of control solutions to those containing MOF was used to determine the amount of selenate or selenite adsorbed by the MOF at each time. Studies at 40 °C and pH 6 were performed in the same fashion. To perform tests at 40 °C, the selenate and selenite solutions were heated in a beaker full of Lab Armor Beads, and to perform tests at pH 6, the selenate and selenite solutions were made in pH 6 HCl.

NU-1000 Adsorption Studies per Gram. The amount of selenate or selenite adsorbed per gram of NU-1000 was determined by exposing 5 mg of NU-1000 to 10 mL of an aqueous solution of selenium as sodium selenite or sodium selenate in a 15 mL polypropylene centrifuge tube with concentrations of ca. 18, 27, 36, , and 55 ppm. These concentrations correspond to an exposure level of 1.00, 1.50, 2.00, 2.50, and 3.00 analyte molecules per Zr_6-node of NU-1000. The solutions were centrifuged for 30 s to allow the MOF to settle to the bottom of the tube. Aliquots of the supernatant were removed and diluted to 10 mL in 3% H_2SO_4 at 1, 2, 3, 4, 5, 10, 15, 30, 60, 90, 120, and 180 min for analysis by ICP-OES. ICP-OES was used to determine the concentration of Se, Zr, and Na in each solution. Comparison of control solutions to those containing MOF was used to determine the amount of selenate or selenite adsorbed (q) in mg/g of NU-1000 where $q = (C_i - C_f) \times V/m$, C_i = initial concentration, C_f = final concentration, V = volume of solution exposed to NU-1000, and m = mass of NU-1000 in grams.

■ ASSOCIATED CONTENT

Supporting Information

Adsorption capacity data, PXRD patterns, nitrogen adsorption isotherms and pair distribution function analysis data. The Supporting Information is available free of charge on the ACS Publications website at DOI: 10.1021/jacs.5b03904.

■ AUTHOR INFORMATION

Corresponding Author

*o-farha@northwestern,edu

Present Address

[⊥]Michael J. Katz: Department of Chemistry, Memorial University of Newfoundland, St. Johns, NL, A1B, 3X7, Canada.

Author Contributions

[∥]These authors contributed equally.

Notes

The authors declare no competing financial interest.

■ ACKNOWLEDGMENTS

This work was funded through a contract with the Electric Power Research Institute (EPRI). The authors wish to acknowledge technical contributions from EPRI's Dan Wells, Paul Frattini, and Keith Fruzzetti. A.E.P.-P. acknowledges a Beatriu de Pinós fellowship (BP-DGR 2014) from the Ministry of Economy and Knowledge (Catalan Government). Work done at Argonne was performed using the Advanced Photon Source, a U.S. Department of Energy (DOE) Office of Science User Facility operated for the DOE Office of Science by Argonne National Laboratory under Contract No. DE-AC02-06CH11357.

■ REFERENCES

(1) (a) World Health Organization. *Trace Elements in Human Nutrition and Health*; World Health Organization: Geneva, 1996. (b) Chapman, P. M. *Hum. Ecol. Risk Assess.* **1999**, *5*, 1123−1138. (c) Fordyce, F. M. Selenium Deficiency and Toxicity in the Environment. In *Essentials of Medical Geology: Revised Edition*; Selinus, O., Alloway, B., Centeno, J. A., Finkelman, R. B., Fuge, R., Lindh, U., Smedley, P., Eds.; Elsevier: London, 2005; pp 375−416.

(2) Lemly, A. D. *Ecotoxicol. Environ. Saf.* **2004**, *59*, 44−56.

(3) United States Environmental Protection Agency. Basic Information about Selenium in Drinking Water. http://water.epa.gov/drink/contaminants/basicinformation/selenium.cfm (accessed Nov 2014).

(4) Plant, J. A.; Kinniburgh, D. G.; Smedley, P. L.; Fordyce, F. M.; Klinck, B. A. *Treatise Geochem.* **2003**, *9*, 17−66.

(5) Mooney, F. D.; Murray-Gulde, C. *Environ. Geosci.* **2008**, *15*, 131−141.

(6) Luo, Q.; Tsukamoto, T. K.; Zamzow, K. L.; Miller, G. C. *Mine Water Environ.* **2008**, *27*, 100−108.

(7) (a) Balistrieri, L. S.; Chao, T. T. *Soil Sci. Soc. Am. J.* **1987**, *51*, 1145−1151. (b) Balistrieri, L. S.; Chao, T. T. *Geochim. Cosmochim. Acta* **1990**, *54*, 739−751. (c) Duc, M.; Lefèvre, G.; Fédoroff, M.; Jeanjean, J.; Rouchaud, J. C.; Monteil-Rivera, F.; Dumonceau, J.; Milonjic, S. *J. Environ. Radioact.* **2003**, *70*, 61−72. (d) Mitchell, K.; Couture, R.-M.; Johnson, T. M.; Mason, P. R. D.; Van Cappellen, P. *Chem. Geol.* **2013**, *342*, 21−28.

(8) (a) Hayes, K.; Roes, A.; Brown, G.; Hodgson, K.; Leckie, J.; Parks, G. *Science* **1987**, *238*, 783−786. (b) Davis, J. A.; Leckie, J. O. Speciation of adsorbed ions at the oxide/water interface. In *Chemical Modeling in Aqueous Systems: Speciation, Sorption, Solubility and Kinetics*; Jenne, E. A., Ed.; American Chemical Society Symposium Series 93; American Chemical Society: Washington, DC, 1979; pp 299−317.

(9) Farha, O. K.; Eryazici, I.; Jeong, N. C.; Hauser, B. G.; Wilmer, C. E.; Sarjeant, A. A.; Snurr, R. Q.; Nguyen, S. T.; Yazaydın, A. Ö.; Hupp, J. T. *J. Am. Chem. Soc.* **2012**, *134*, 15016−15021.

(10) (a) Gutov, O. V.; Bury, W.; Gomez-Gualdron, D. A.; Krungleviciute, V.; Fairen-Jimenez, D.; Mondloch, J. E.; Sarjeant, A. A.; Al-Juaid, S. S.; Snurr, R. Q.; Hupp, J. T.; Yildirim, T.; Farha, O. K. *Chem.—Eur. J.* **2014**, *20*, 12389−12393. (b) Wang, T. C.; Bury, W.; Gómez-Gualdrón, D. A.; Vermeulen, N. A.; Mondloch, J. E.; Deria, P.; Zhang, K.; Moghadam, P. Z.; Sarjeant, A. A.; Snurr, R. Q.; Stoddart, J. F.; Hupp, J. T.; Farha, O. K. *J. Am. Chem. Soc.* **2015**, *137*, 3585−3591.

(11) (a) Lee, J.; Farha, O. K.; Roberts, J.; Scheidt, K.; Nguyen, S. T.; Hupp, J. T. *Chem. Soc. Rev.* **2009**, *38*, 1450−1459. (b) Gascon, J.; Corma, A.; Kapteijn, F.; Llabrés i Xamena, F. X. *ACS Catal.* **2014**, *4*, 361−378.

(12) Kreno, L. E.; Leong, K.; Farha, O. K.; Allendorf, M.; Van Duyne, R. P.; Hupp, J. T. *Chem. Rev.* **2012**, *112*, 1105−1125.

(13) (a) Dincă, M.; Long, J. R. *Angew. Chem., Int. Ed.* **2008**, *47*, 6766−6779. (b) Li, J.-R.; Kuppler, R. J.; Zhou, H.-C. *Chem. Soc. Rev.* **2009**, *38*, 1477−1504. (c) Farha, O. K.; Yazaydın, A. Ö.; Eryazici, I.; Malliakas, C. D.; Hauser, B. G.; Kanatzidis, M. G.; Nguyen, S. T.; Snurr, R. Q.; Hupp, J. T. *Nat. Chem.* **2010**, *2*, 944−948.

DOI: 10.1021/jacs.5b03904
J. Am. Chem. Soc. 2015, 137, 7488−7494

(14) (a) Barea, E.; Montoro, C.; Navarro, J. A. R. *Chem. Soc. Rev.* **2014**, *43*, 5419−5430. (b) DeCoste, J. B.; Peterson, G. W. *Chem. Rev.* **2014**, *114*, 5695−5727. (c) Khan, N. A.; Hasan, Z.; Jhung, S. H. *J. Hazard. Mater.* **2013**, *244*−*245*, 444−456.
(15) (a) Férey, G. *Chem. Soc. Rev.* **2007**, *37*, 191−214. (b) Furukawa, H.; Cordova, K. E.; O'Keefe, M. O.; Yaghi, O. M. *Science* **2013**, *341*, 1230444. (c) Jiang, H.-L.; Xu, Q. *Chem. Commun.* **2011**, *47*, 3351−3370.
(16) (a) Cavka, J. H.; Jakobsen, S.; Olsbye, U.; Guillou, N.; Lamberti, C.; Bordiga, S.; Lillerud, K. P. *J. Am. Chem. Soc.* **2008**, *130*, 13850−13851. (b) Valenzano, L.; Civalleri, B.; Chavan, S.; Bordiga, S.; Nilsen, M. H.; Jakobsen, S.; Lillerud, K. P.; Lamberti, C. *Chem. Mater.* **2011**, *23*, 1700−1718. (c) Katz, M. J.; Brown, Z. J.; Colón, Y. J.; Siu, P. W.; Scheidt, K. A.; Snurr, R. Q.; Hupp, J. T.; Farha, O. K. *Chem. Commun.* **2013**, *49*, 9449−9451.
(17) Wu, H.; Chua, Y. S.; Krungleviciute, V.; Tyagi, M.; Chen, P.; Yildirim, T.; Zhou, W. *J. Am. Chem. Soc.* **2013**, *135*, 10525−10532.
(18) Ruvarac, A. Group IV Hydrous Oxides—Synthetic Inorganic Ion Exchangers. In *Inorganic Ion Exchange Materials*; Clearfield, A., Ed.; CRC Press: Boca Raton, FL, 1982; pp 141−160.
(19) (a) Suzuki, T. M.; Bomani, J. O.; Matsunaga, H.; Yokoyama, T. *React. Funct. Polym.* **2000**, *43*, 165−172. (b) Suzuki, T. M.; Tanco, M. L.; Pacheco Tanaka, D. A.; Matsunaga, H.; Yokoyama, T. *Sep. Sci. Technol.* **2001**, *36*, 103−111. (c) Peräniemi, S.; Hannonen, S.; Mustalahti, H.; Ahlgrén, M. *Fresenius' J. Anal. Chem.* **1994**, *349*, 510−515. (d) Biswas, B. K.; Inoue, K.; Kawakita, H.; Harada, H.; Ohto, K.; Alam, S. *J. Water Environ. Technol.* **2010**, *8* (4), 313−320. (e) Yuchi, A.; Matsuo, K. *J. Chromatogr., A* **2005**, *1082*, 208−213.
(20) Planas, N.; Mondloch, J. E.; Tussupbayev, S.; Borycz, J.; Gagliardi, L.; Hupp, J. T.; Farha, O. K.; Cramer, C. J. *J. Phys. Chem. Lett.* **2014**, *5*, 3716−3723.
(21) Moyer, B. A.; Custelcean, R.; Hay, B. P.; Sessler, J. L.; Bowman-James, K.; Day, V. W.; Kang, S.-O. *Inorg. Chem.* **2013**, *52*, 3473−3490.
(22) (a) Deria, P.; Mondloch, J. E.; Tylianakis, E.; Ghosh, P.; Bury, W.; Snurr, R. Q.; Hupp, J. T.; Farha, O. K. *J. Am. Chem. Soc.* **2013**, *135*, 16801−16804. (b) Deria, P.; Bury, W.; Hupp, J. T.; Farha, O. K. *Chem. Commun.* **2014**, *50*, 1965−1968. (c) Deria, P.; Bury, W.; Hod, I.; Kung, C.-W.; Karagiaridi, O.; Hupp, J. T.; Farha, O. K. *Inorg. Chem.* **2015**, *54*, 2185−2192. (d) Deria, P.; Mondloch, J. E.; Karagiaridi, O.; Bury, W.; Hupp, J. T.; Farha, O. K. *Chem. Soc. Rev.* **2014**, *43*, 5896−5912.
(23) Mondloch, J. E.; Bury, W.; Fairen-Jimenez, D.; Kwon, S.; DeMarco, E. J.; Weston, M. H.; Sarjeant, A. A.; Nguyen, S. T.; Stair, P. C.; Snurr, R. Q.; Farha, O. K.; Hupp, J. T. *J. Am. Chem. Soc.* **2013**, *135*, 10294−10297.
(24) Yang, Q.; Wiersum, A. D.; Llewellyn, P. L.; Guillerm, V.; Serred, C.; Maurin, G. *Chem. Commun.* **2011**, *47*, 9603−9605.
(25) Cramer, C.; Price, D. L.; Saboungi, M.-L. *J. Phys.: Condens. Matter* **1998**, *10*, 6229−6242.
(26) Vlaev, L. T.; Genieva, S. D. *J. Struct. Chem.* **2004**, *45*, 825−831.
(27) Electric Power Research Institute. Identification of Unknown Selenium Species in Flue Gas Desulfurization Water. http://www.epri.com/abstracts/Pages/ProductAbstract.aspx?ProductId=000000000001014944.
(28) (a) Chan, Y. T.; Kuan, W. H.; Chen, T. Y.; Wang, M. K. *Water Res.* **2009**, *43*, 4412−4420. (b) Bleiman, N.; Mishael, Y. G. *J. Hazard. Mater.* **2010**, *183*, 590−595. (c) Yamani, J. S.; Lounsbury, A. W.; Zimmerman, J. B. *Water Res.* **2014**, *50*, 373−381. (d) Nishimura, T.; Hashimoto, H.; Nakayama, M. *Sep. Sci. Technol.* **2007**, *42*, 3155−3167. (e) Suzuki, T. M.; Pacheco Tanaka, D. A.; Llosa Tanco, M. A.; Kanesato, M.; Yokoyama, T. *J. Environ. Monit.* **2000**, *2*, 550−555. (f) Mandal, S.; Mayadevi, S.; Kulkarni, B. D. *Ind. Eng. Chem. Res.* **2009**, *48*, 7893−7898. (g) Tuzen, M.; Sari, A. *Chem. Eng. J.* **2010**, *158*, 200−206. (h) Yokoi, T.; Tatsumi, T.; Yoshitake, H. *Bull. Chem. Soc. Jpn.* **2003**, *76*, 2225−2232.
(29) Mavrov, V.; Stamenov, S.; Todorova, E.; Chmiel, H.; Erwe, T *Desalination* **2006**, *201*, 290−296.
(30) (a) Hammersley, A. P. ESRF Internal Report, **ESRF97HA02T**, *FIT2D: An Introduction and Overview*, 1997. (b) Hammersley, A. P.; Svensson, S. O.; Hanfland, M.; Fitch, A. N.; Häusermann, D. *High Pressure Res.* **1996**, *14*, 235−248.
(31) Juhás, P.; Davis, T.; Farrow, C. L.; Billinge, S. J. L. *J. Appl. Crystallogr.* **2013**, *46*, 560−566.
(32) Farrow, C. L.; Juhás, P.; Liu, J. W.; Bryndin, D.; Bŏzin, E. S.; Bloch, J.; Proffen, Th.; Billinge, S. J. L. *J. Phys.: Condens. Matter* **2007**, *19*, 335219.
(33) (a) Jun, J. W.; Tong, M.; Jung, B. K.; Hasan, Z.; Zhong, C.; Jhung, S. H. *Chem. Eur. J.* **2015**, *21*, 347−354. (b) Tong, M.; Liu, D.; Yang, Q.; Devautour-Vinot, S.; Maurin, G.; Zhong, C. *J. Mater. Chem. A* **2013**, *1*, 8534−8537.

DOI: 10.1021/jacs.5b03904
J. Am. Chem. Soc. 2015, 137, 7488−7494